

Sawteeth and 1/1 modes

Linda Sugiyama

Laboratory for Nuclear Science
Massachusetts Institute of Technology

CEMM Meeting
Int'l Sherwood Theory Conference
Santa Fe NM
April 14, 2013

Topics

- Compressibility and finite aspect ratio corrections drastically change the $m=1, n=1$ MHD internal kink mode in a torus – better resembles experiments
 - Large aspect ratio and full MHD very different from RMHD
 - Compressible changes start in the linear 1/1 mode
 - Nonlinear MHD: X-layer, not Sweet-Parker reconnection!
Fast crash phase with fast onset; rate nearly independent of η .
 - Large aspect ratio expansion breaks down nonlinearly at small $r_1/R \approx 1/10$
- Compressibility \leftrightarrow evolving dn/dt
- New type of nonlinear 1/1 "snake" mode with a finite size density perturbation at $q=1$ resembles the early stage of heavy-impurity ion snakes in Alcator C-Mod

Compressible 1/1 internal kink in a torus

- Compressibility changes the $m=1, n=1$ MHD internal kink in a torus, linearly and nonlinearly
- Original toroidal large aspect ratio solution for linear 1/1 ideal MHD internal kink mode was incompressible (Bussac, 1975)
- Compressible large aspect ratio analytical linear mode solution exists (Wahlberg, J. Pl. Phys. 1999, done with symbolic algebra program), but hard to interpret.
- Nonlinear instability has been analyzed with RMHD, assuming linear mode 1/1 eigenfunction form and dropping higher order aspect ratio terms
 - Hazeltine, et al., PF 1986 neglected current in $q=1$ layer: exponential mode growth at $\gamma \lesssim \gamma_L$
 - Waelbrock, PF B 1989 used 1/1 magnetic island and helical magnetic flux conservation: modified Sweet-Parker reconnection layer and island width $W \sim \eta t^2$
 - Biskamp, PF B 1991 used 1/1 island and linear eigenfunction: Result similar to Waelbrock. Showed corresponding poloidal stream function growth $U \sim \eta t$ matched the numerical RMHD solution.

- Problem: $W \sim \eta t^2$ growth is too slow to explain observed the speed of sawtooth crashes in later plasmas at smaller resistivities
- One solution: outside MHD, nonlinear electron effects, parallel electron compressibility or electron inertia or other kinetic effects. can greatly speed up the instability (eg, Ayedmir PoP 1991, Wang PRL 1992).
 - These widen and shorten the narrow, poloidally elongated Sweet-Parker reconnection layer to an “X” shape.
- But **non-MHD effects are NOT needed for fast crash!**
 - RMHD model strongly constrains the perturbations to $m_0=1$, $n_0=1$ and $m=n$. This leads to formation of a narrow, poloidally elongated ($\theta \lesssim 0.8\pi/2$) reconnection and current layer, which constricts the plasma flow through the layer and reduces the attainable reconnection rate.
 - *Compressible MHD never lets a Sweet-Parker type layer develop*, due to the presence of $m=2,0$ $n=1$ harmonics from the linear mode.

Compressible large aspect ratio MHD model

$$\mathbf{v} = \epsilon R \nabla_{\perp} U \times \hat{\phi} + \nabla_{\perp} \chi + V \hat{\phi} \quad (1)$$

$$\mathbf{B} = \nabla_{\perp} \psi \times \nabla \phi + (1/R) \nabla_{\perp} F + (I/R) \hat{\phi} \quad (2)$$

$$d\psi/dt = \partial U / \partial \phi + \eta \nabla_{\perp}^2 \psi \quad (3)$$

$$dw/dt = -(1/\rho) \mathbf{B} \cdot \nabla J_{\phi} - Yw + \mu \nabla^2 w \quad (4)$$

$$dp/dt = -\Gamma Y p + \nabla \cdot n \boldsymbol{\kappa}_T \cdot \nabla (p/n) \quad (5)$$

$$dI/dt = \mathbf{B}_{\perp} \cdot \nabla_{\perp} V - YI + \eta \nabla_{\perp}^2 I \quad (6)$$

$$dV/dt = (1/\rho) \mathbf{B}_{\perp} \cdot \nabla_{\perp} I - (1/\rho) \partial p / \partial \phi + \mu \nabla^2 V \quad (7)$$

$$w \equiv -\hat{\phi} \cdot \nabla \times \mathbf{v} = \nabla_{\perp}^2 U + (1/R) \partial U / \partial R \quad (8)$$

$$Y \equiv \nabla \cdot \mathbf{v}_{\perp} = y + z \quad (9)$$

$$y = \nabla_{\perp}^2 \chi + (1/R) \partial \chi / \partial R \quad (10)$$

$$z = -2\epsilon (\partial U / \partial Z) \quad (11)$$

$$R J_{\phi} = -\nabla_{\perp}^2 \psi + (1/R) \partial \psi / \partial R - (1/R) \partial F / \partial Z \quad (12)$$

$$d/dt = (\partial / \partial t) + \mathbf{v} \cdot \nabla \quad (13)$$

Compressible large aspect ratio MHD -2-

An equation for χ can be written from $\nabla r \cdot \partial \mathbf{v}_\perp / \partial t$ as

$$\begin{aligned} \partial(\chi' + U') / \partial t &= -(v_\perp^2 / 2)' + (1/\rho) [-(I^2 / 2)' - p' + J_\phi \psi' / R] \\ &\quad + w(U' - \chi') + \mu \nabla^2 (\chi' + U'). \end{aligned} \quad (1)$$

where the “radial” and “poloidal” derivatives are $f' \equiv \nabla r \cdot \nabla_\perp f$ and $f^\wedge \equiv \nabla r \times \nabla_\perp f \cdot \hat{\phi}$ for generalized radial and poloidal coordinates.

The equation for the compressibility shows that linearly the main terms are related to χ , not U ($\hat{y} \equiv \nabla_\perp^2 \chi$)

$$\begin{aligned} \frac{\partial \hat{y}}{\partial t} &= -\frac{1}{\rho} \left[\nabla_\perp \cdot \frac{J_\phi}{R} \nabla_\perp \psi - \nabla_\perp^2 \left(p + \frac{I^2}{2} \right) \right] - \nabla_\perp^2 \frac{v_\perp^2}{2} \\ &\quad + \nabla_\perp \cdot (w \nabla_\perp U) - \nabla_\perp \chi \times \nabla_\perp w \cdot \hat{\phi} + \mu \nabla^2 \hat{y}. \end{aligned} \quad (2)$$

Linear mode compressibility

Linear analysis

If $\tilde{B}_{\parallel} = 0$, can show that the compressibility

$$\nabla \cdot \mathbf{v}_{\perp} = -2\epsilon \mathbf{v}_{\perp} \cdot \boldsymbol{\kappa} \simeq -2\epsilon(\partial U / \partial Z). \quad (1)$$

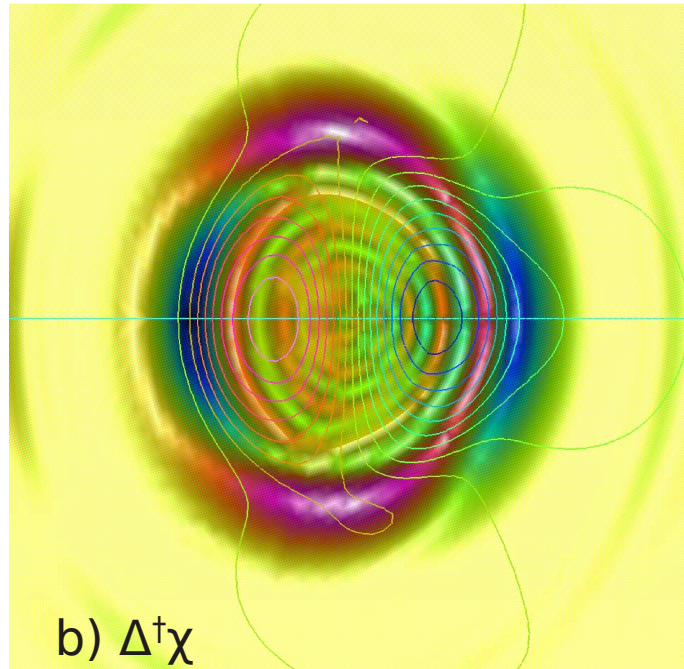
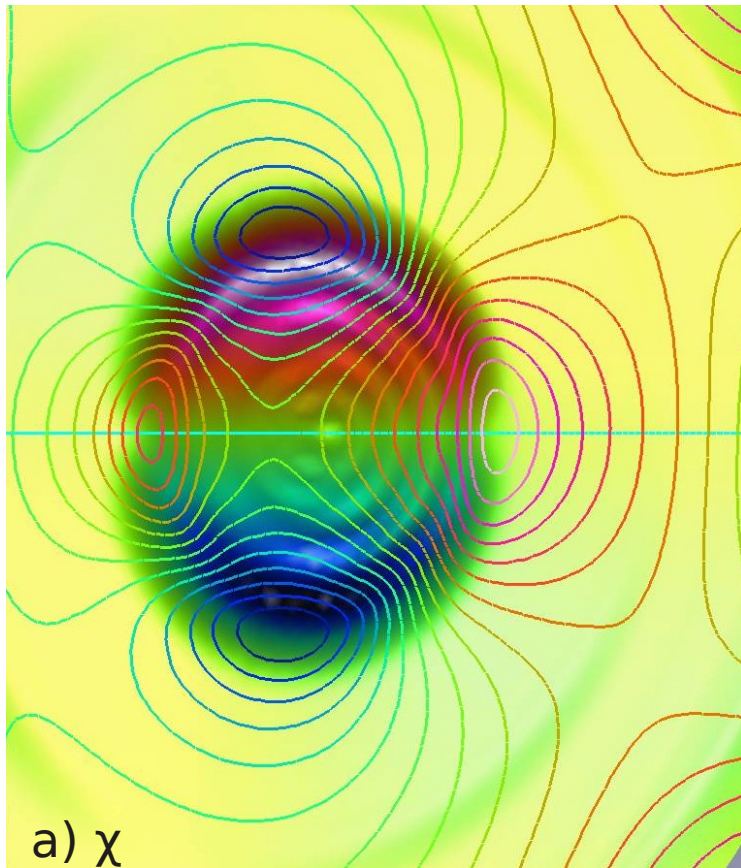
Leads to components $v_{\phi}^{m=0}$ and $v_{\phi}^{m=2}$ representing the “sound wave” terms. The $m \neq 1$ v_{ϕ} and $\nabla \cdot \boldsymbol{\xi}_{\perp}$ contribute to δW and contribute to a linear growth rate scaling $\gamma \sim \epsilon \beta_p$.

If $\tilde{B}_{\parallel} \neq 0$, $\chi^{m=2}$ enters through $y = \nabla \cdot \nabla_{\perp} \chi$ (note $\chi^{m=1} < \chi^{m=2}$). This introduces the “compressional Alfvén wave” coupling of v_{ϕ} , p , I . All the CLAR equations couple to create a 2nd order PDE for χ .

Analysis simpler than Wahlberg '99 - expands around the actual magnetic axis instead of unshifted circular equilibrium.

Nonlinearly, the higher m 's localize the layer poloidally near the X-point and prevent the elongated Sweet-Parker layer from developing.

Compressible χ component is $m=2, n=1$



- a) Lines show χ , shaded red/blue U , poloidal stream function.
 $m=1$ U gives main radial displacement over $0 < q < 1$, $v_r = \gamma \xi_r^1 \approx U^1/r$.
- b) Red, blue shading shows $y = \nabla \cdot \nabla_{\perp} \chi$ is large and predominantly $m=2$ at $q=1$. Contour lines are ψ .

MHD vs Large aspect ratio and RMHD

Perpendicular (\perp to ϕ) momentum equation, neglecting viscosity,

$$\rho(\partial \mathbf{v}_{\perp} / \partial t) = -\rho(\mathbf{v} \cdot \nabla) \mathbf{v}_{\perp} + (\rho v_{\phi}^2 / R) \hat{\mathbf{R}} + (\mathbf{J} \times \mathbf{B} - \nabla p)_{\perp} = \mathbf{M}. \quad (1)$$

Left hand side:

$$\text{LargeAspectRatio} \quad \mathbf{M}_L = \mathbf{P} - \mathbf{K} \quad (2)$$

$$\mathbf{P} = \nabla_{\perp} (p + I^2 / 2) + \rho \nabla_{\perp} (v_{\perp}^2 / 2) \quad (3)$$

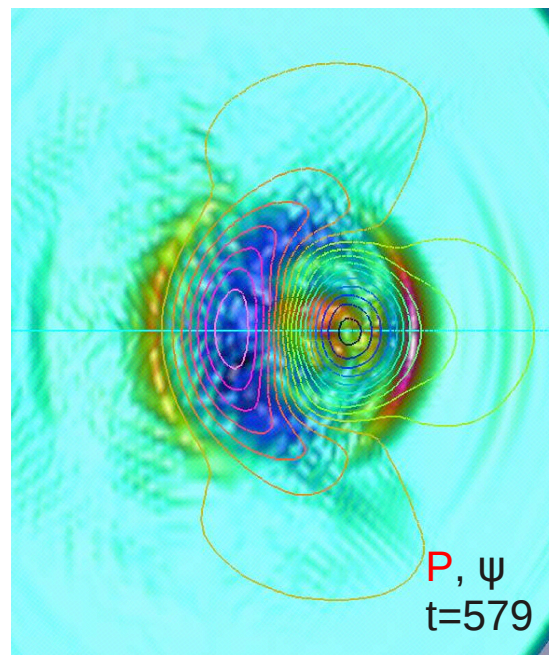
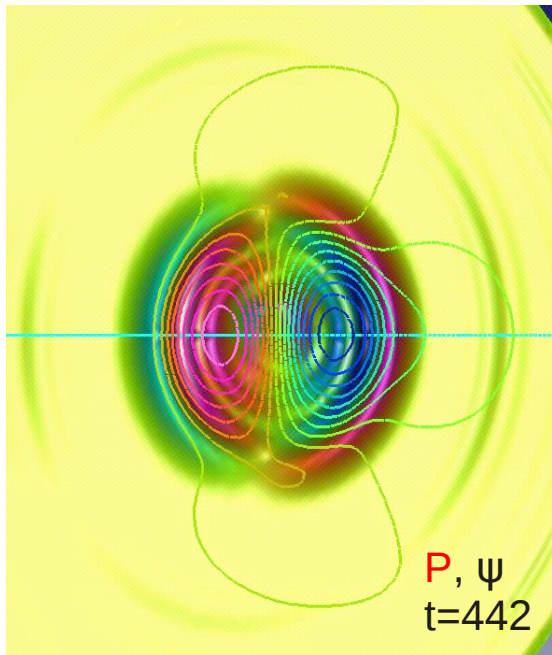
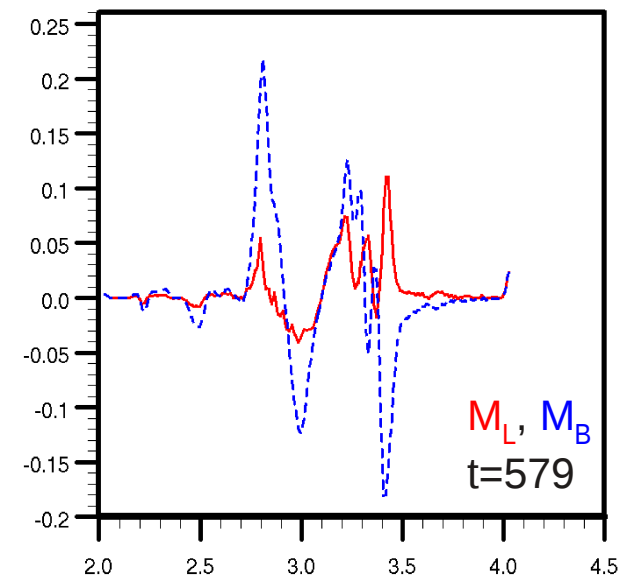
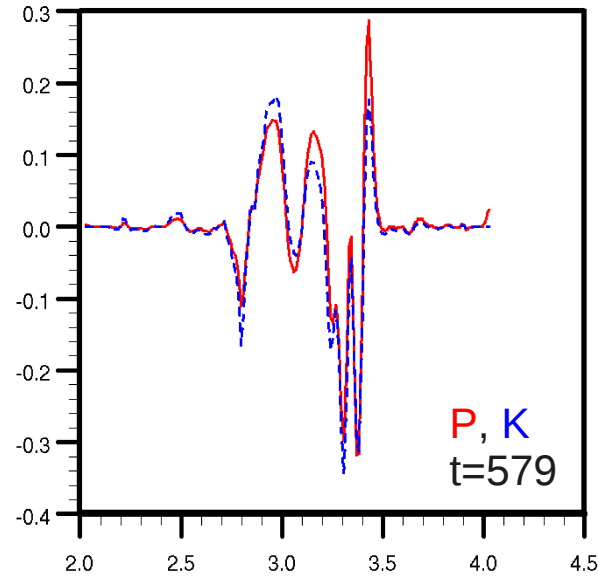
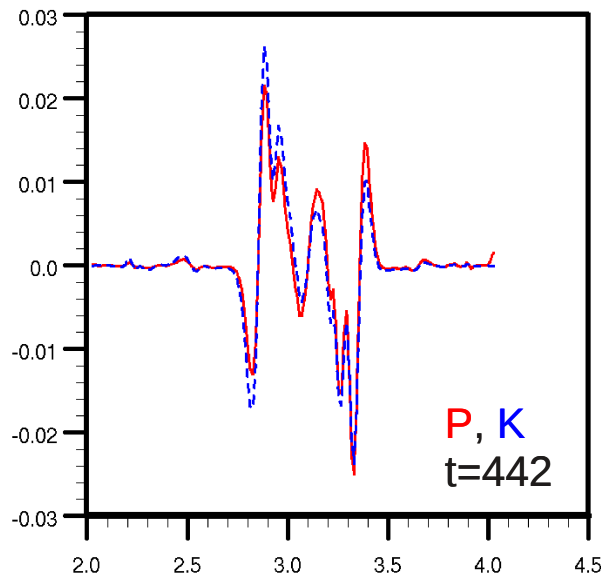
$$\mathbf{K} = (J_{\phi} / R) \nabla_{\perp} \psi \quad (4)$$

$$\text{RMHD (Biskamp 91)} \quad \mathbf{M}_B = \nabla_{\perp} (p + \rho v_{\perp}^2 / 2 + B^2 / 2). \quad (5)$$

Full MHD (radial component):

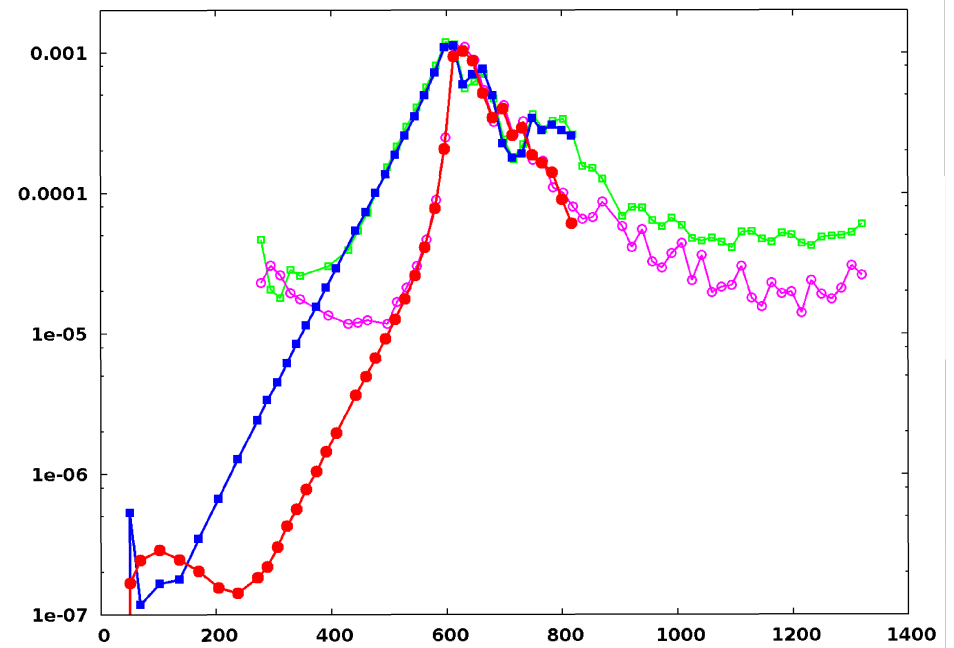
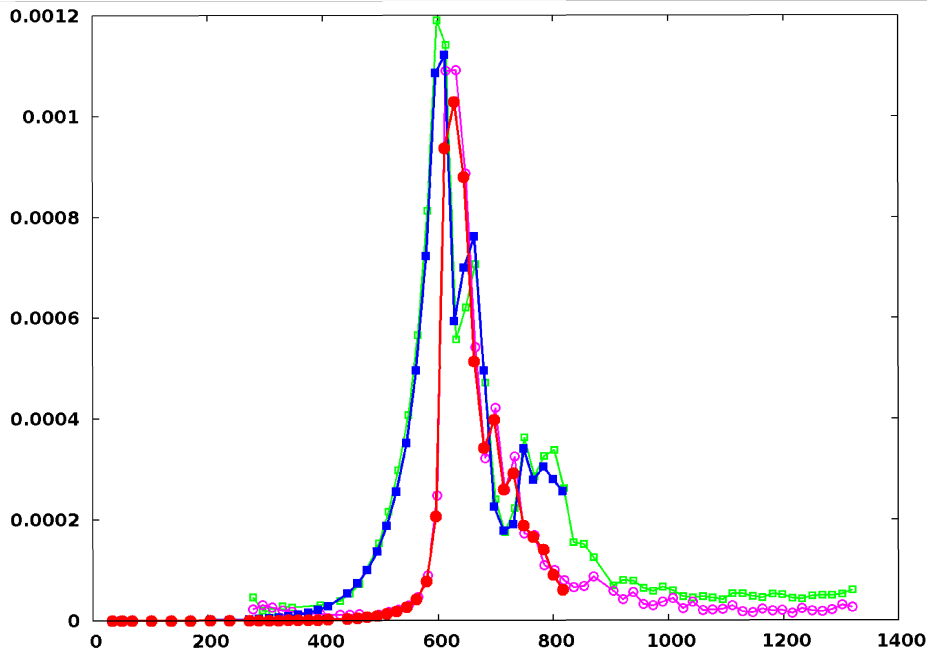
$$\begin{aligned} M_r = & p' + \rho(v_{\perp}^2 / 2)' + (R_o / R)^2 (I^2 / 2)' - (J_{\phi} / R)(\psi' - F') \\ & + \rho(R / R_o) w ((R / R_o) U' - \chi') - \rho(v_{\phi}^2 / R) (\nabla r \cdot \nabla R) \\ & + \rho(v_{\phi} / R) ((\partial \chi / \partial \phi)' + (R / R_o) (\partial U / \partial \phi)') \\ & - (R_o / R)^2 (I / R) ((\partial \psi / \partial \phi)' + (\partial F / \partial \phi)') \\ & - \mu (\nabla^2 \chi' + \nabla^2 U'). \end{aligned} \quad (6)$$

Strong local cancellation occurs in the LAR (and full MHD) perpendicular momentum terms M



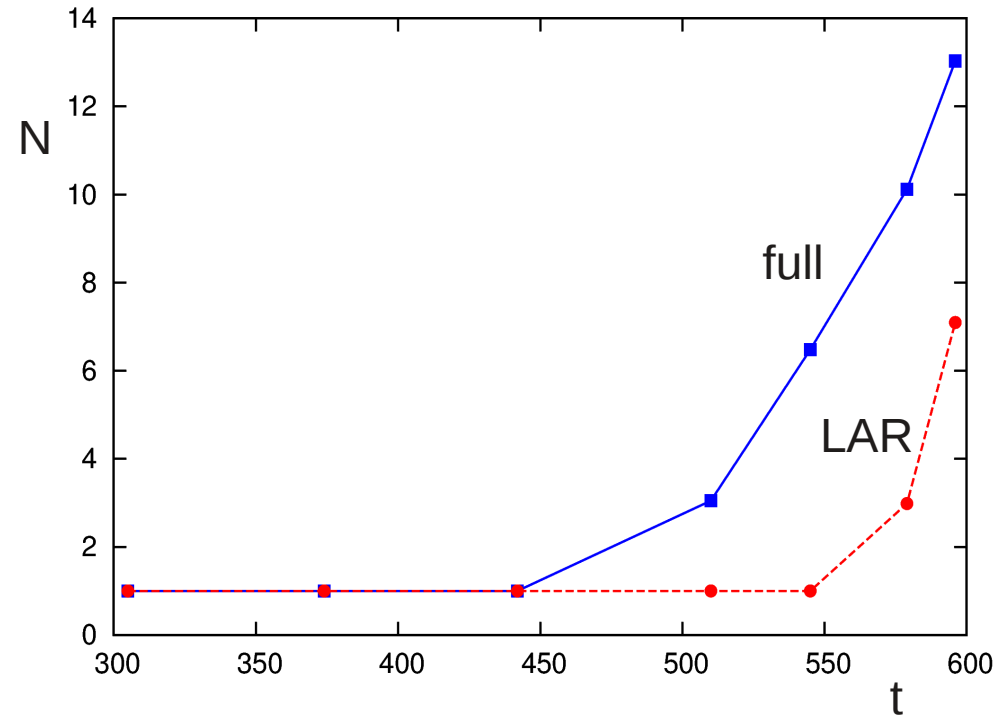
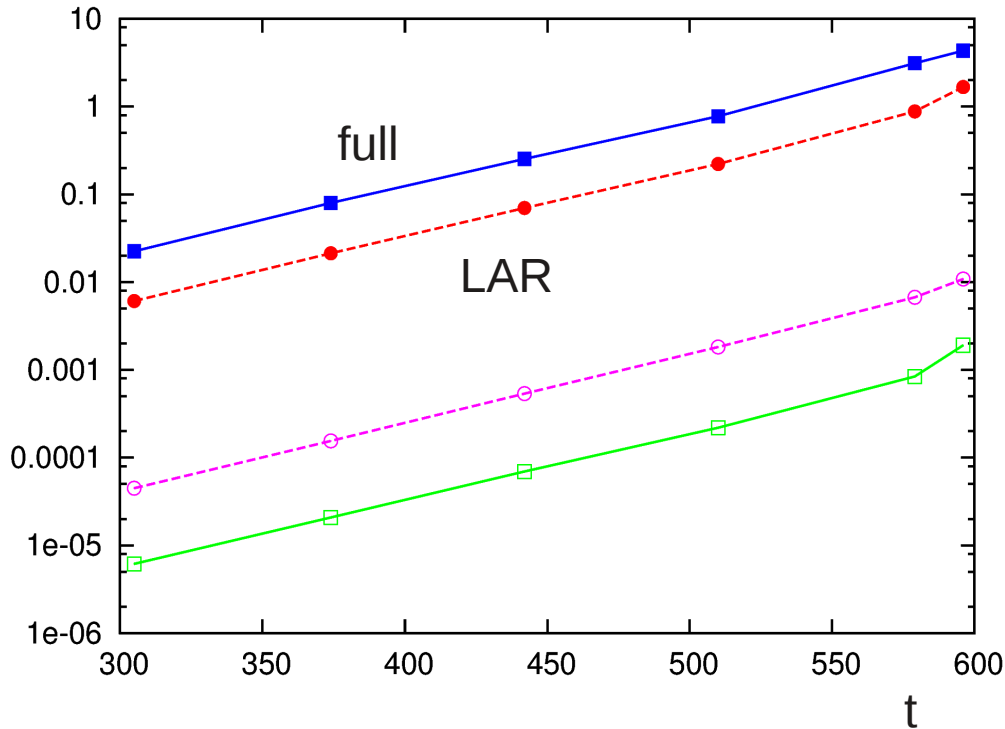
- LAR momentum terms P, K, M shown at early and late times
- Early $t=442$ has no or very small island; $t=579$ has island $W \sim r_1/2$.
- RMHD M_B always has different shape than M or M_L

Time history shows late stage fast crash



- a) Time history of natural and density-triggered crashes at $S=10^6$. Red is U , blue ψ in L2 norm $\|f\|_2 = (\int d^3v |f^2| / \int d^3v)^{1/2}$. Triggered crash is rigidly displaced in time to overlay peak of natural crash (pink/green). Time in τ_A .
- b) Log plot of same.
- Central temperature and $1/1 \psi$ are completely lost at peak amplitude. Central density is lost over next 200-250 τ_A .

Full MHD develops more higher harmonics faster

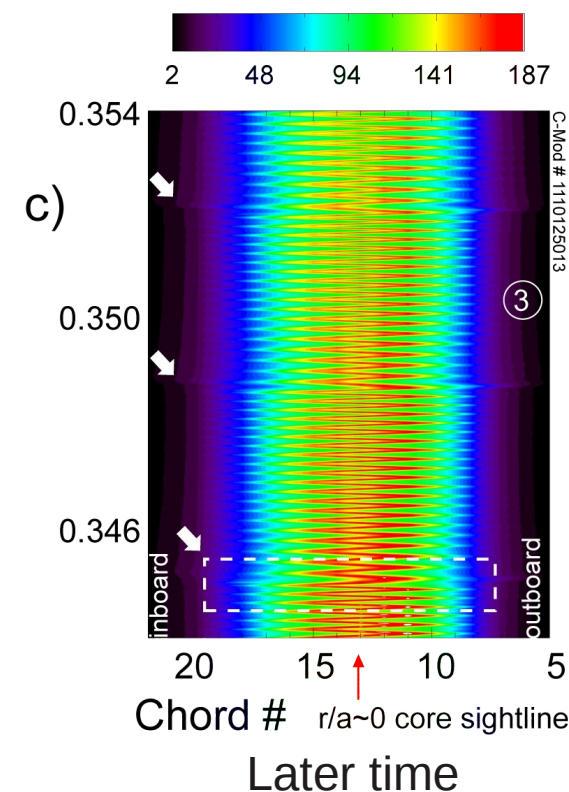
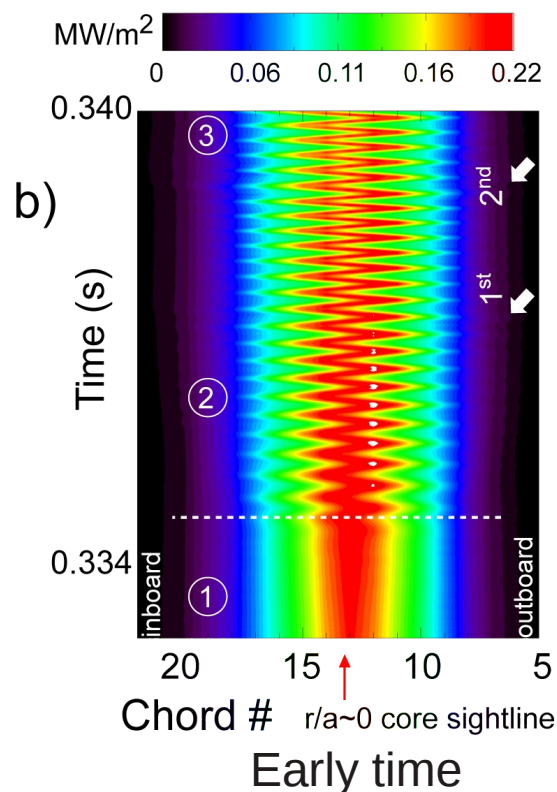
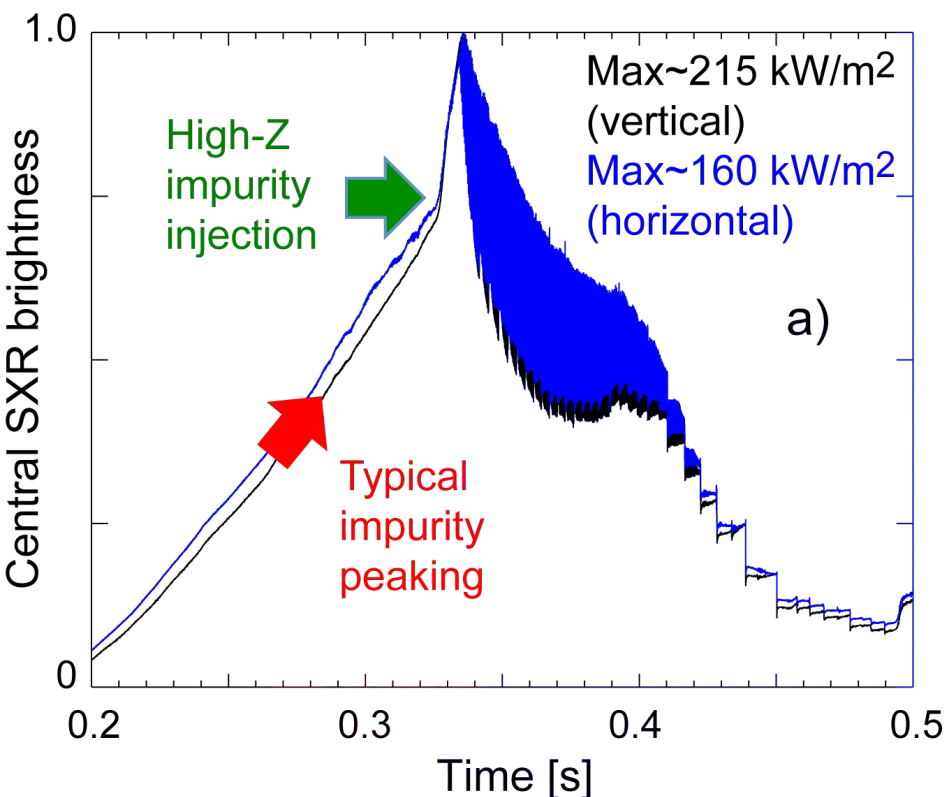


- a) Ratio of $n \geq 2$ harmonics to the $n=1$ (L2 norms) in time for M_r (solid top curve) and M_{Lr} (dashed top curve). $n=1$ value shown in lower two curves.
- Harmonic number N for which at least $\frac{1}{2}$ the total L2 amplitude lies in harmonics $n \geq N$. Full MHD M_r (blue) develops high harmonics much faster than the LAR M_L terms (red), at small island width. ($N=2$ time cannot be computed).

1/1 helical ion density snakes

- Snakes are common long-lived helical concentrations of ion density around magnetic rational surfaces, most often at $q=1$
 - Typically coexist with periodic sawtooth oscillations
 - Variation in ion type, background plasma, formation
- New high resolution observations on Alcator C-Mod show details of heavy-impurity snake formation and interaction with sawtooth oscillations. Simulated with M3D – first results:
 - L. Delgado-Aparicio, L. Sugiyama, et al., PRL 2012
 - L. Delgado-Aparicio, L. Sugiyama, et al., NF 2013
 - L. Sugiyama, PoP 2013.
- Important for ITER
 - $q=1$ radius nearly $a/2$
 - Tungsten $Z=74$ vs C-Mod molybdenum $Z=45$ (32 main charge state in snake) plus diagnostic ions Ar, etc \rightarrow larger δn_e

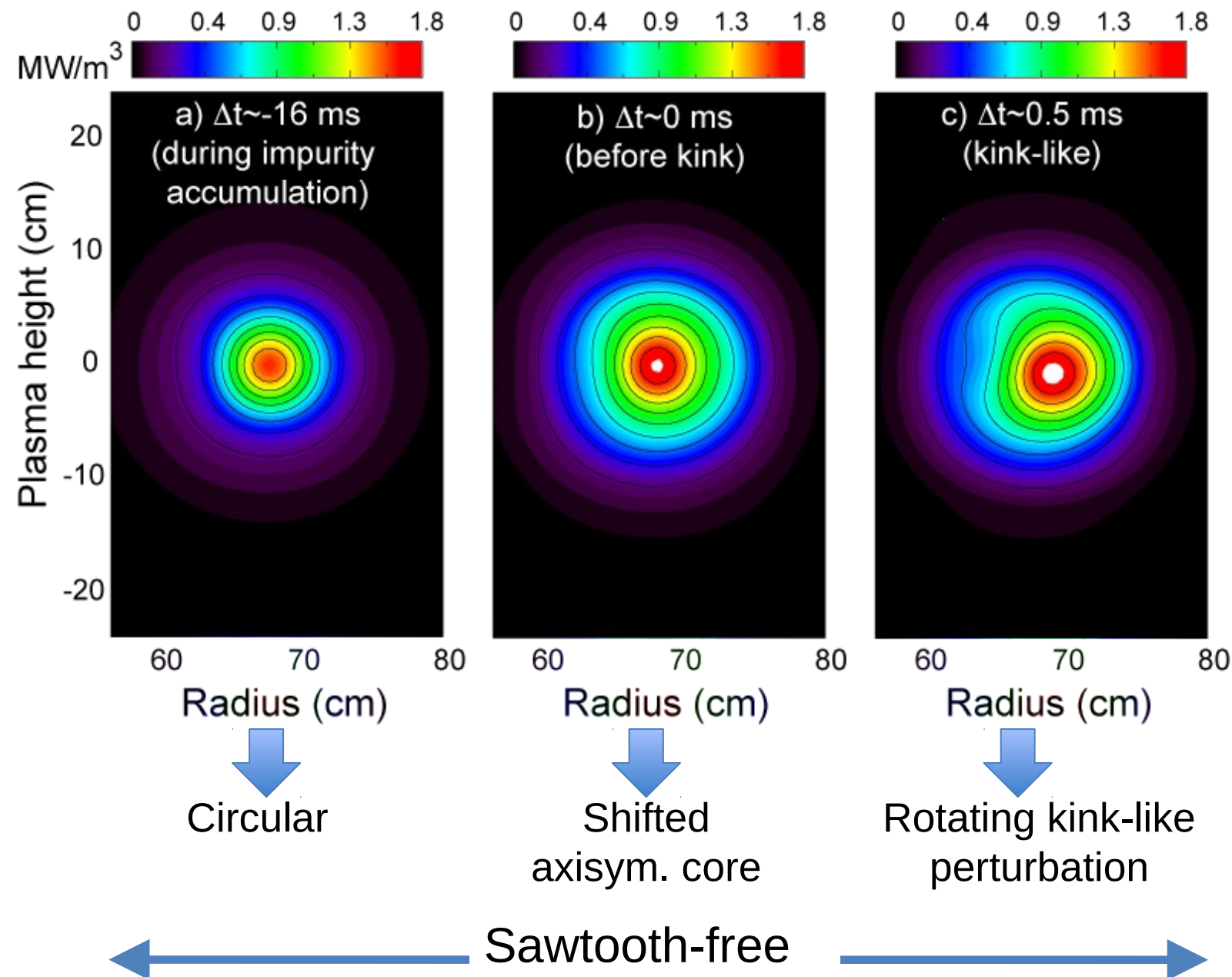
Long-lived (1,1) snake modes in C-Mod are routinely observed on a number of diagnostics



- Ohmic current ramp-up phase or early in the current flattop.
 - High- T_{edge} at startup increases Mo impurity erosion from wall/limiter
 - Impurity density pinch leads to on-axis impurity peaking (axisymmetric)
- 3 stages: Initial central impurity peaking → Broad 1/1 central kink → 1/1 crescent with sawtooth oscillation of core. (Sawtooth crashes shown by arrows.)

Alcator C-Mod early snake: Formation of broad 1/1 kink structure

LDA12: Alcator C-Mod



Mo accumulates in plasma core

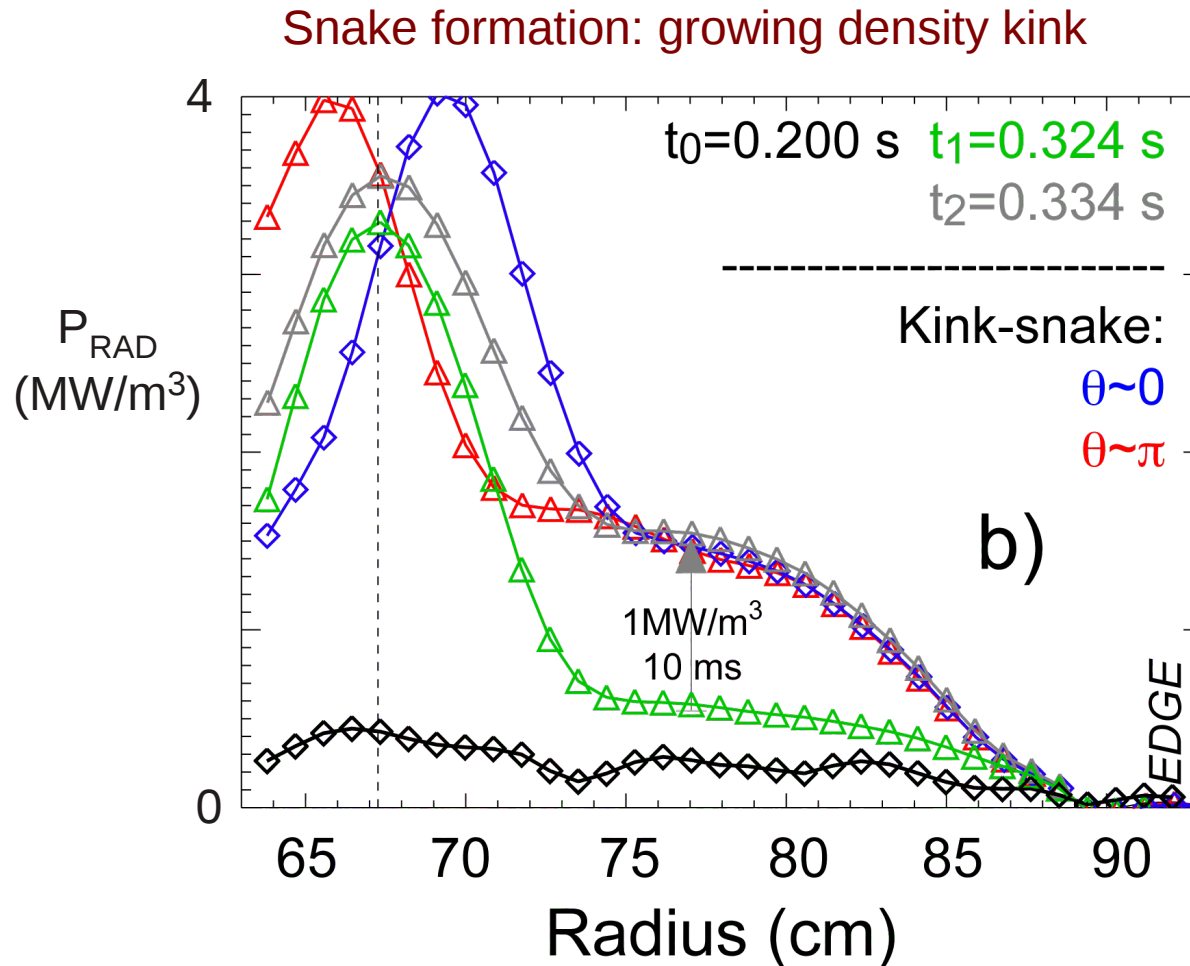
1/1 kink forms

Sawtooth-free early kink-like state lasts from few to hundreds of ms (Continuing impurity-ion pinch?)

First few crashes appear to cause transition to crescent snake inside $q < 1$ (how?)

High-resolution AXUV arrays show growing impurity density kink during snake formation

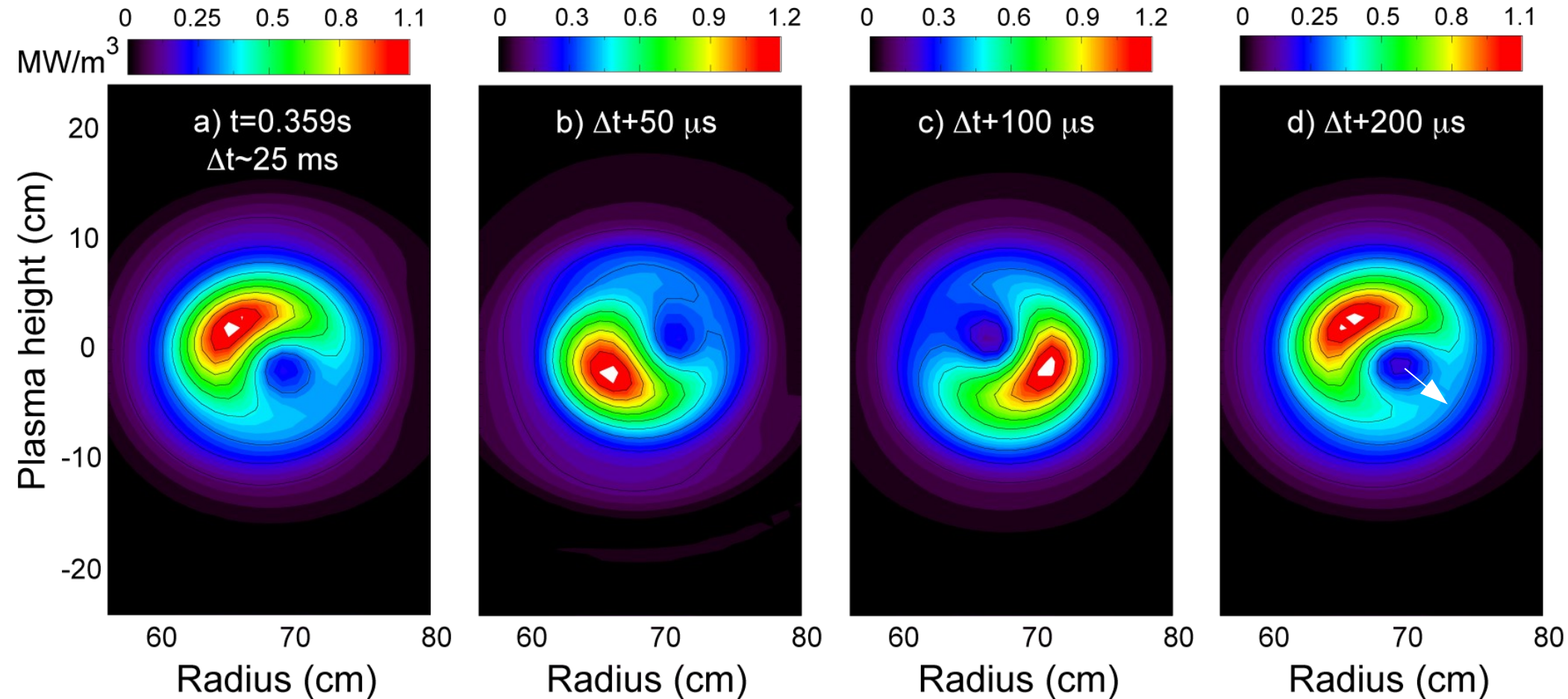
LDA12: Alcator C-Mod



- AXUV P_{rad} measurements show n_{Mo} .
- Allows SXR signal to be identified with impurity density, without T_e contamination (unlike most snake SXR measurements).

Later stage: Crescent-shaped 1/1 “magnetic island”

LDA12: Alcator C-Mod



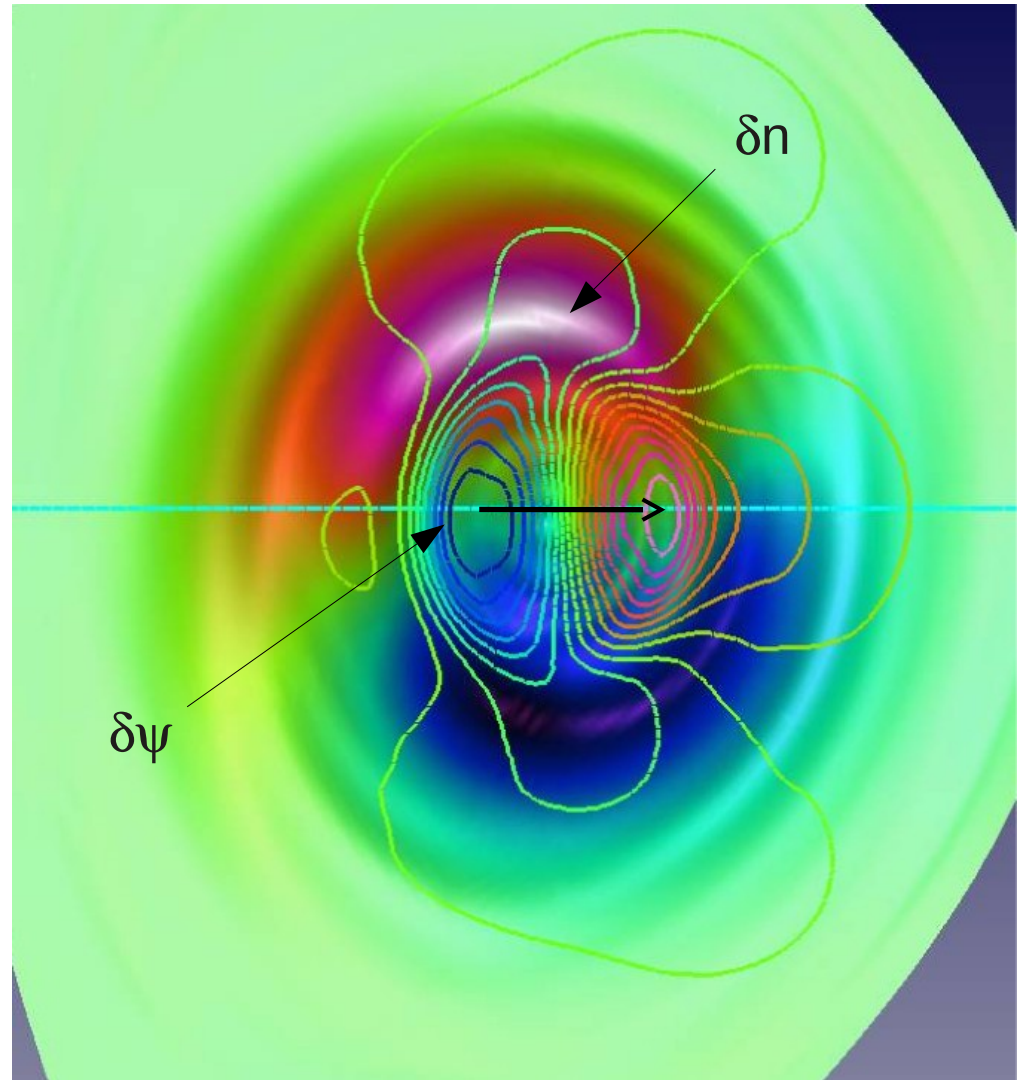
- 1/1 helical structure rotates toroidally with background toroidal rotation (electron diamagnetic direction)
- Periodic partial sawteeth: Dark circular core (low n_{M0} , higher T) rapidly moves outward to $q \approx 1$, then returns inward more slowly to center.

M3D simulation results: $Z\delta n_z = \delta n_e = \delta n_{\text{MHD}}$

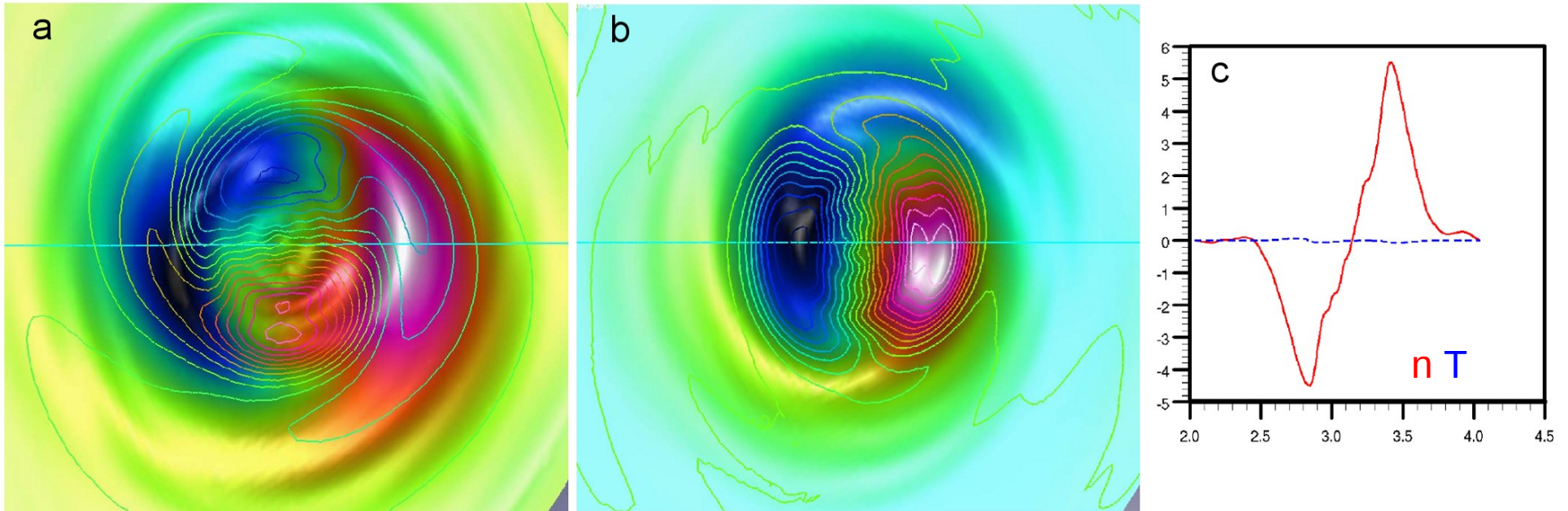
- Snake is a nonlinear dynamic density state.
- Density evolution is crucial.
- Toroidal rotation is important.
- Two δn components: $q \approx 1$, $q < 1$
 - Quasi-steady state helical density concentration around $q=1$ layer (including outside) with small helical δp , since δT evolves to compensate δn . Either helicity $\theta \pm \varphi$. Sustained if small-moderate local q -shear. Similar to W. Cooper's static 3D helical-core equilibria, but self-formed.
 - Helical density at $q=1$ drives a new nonlinear 1/1 internal-kink type perturbation over $q < 1$, very slowly growing. δn anti-aligned to δp .
 - $q < 1$ kink motion is perpendicular to density concentration at $q=1$, so a sawtooth would not destroy the snake.
 - 1/1 mode also has convective motion aligned with the kink p, ψ . Here, driven by v_φ rotation, larger than kink motion.
- Best fit to early C-Mod impurity snake has applied-density helicity aligned with \mathbf{B} and background toroidal rotation of magnitude similar to experiment. Snake rotates with plasma.

New nonlinear 1/1 mode resembles early stage of C-Mod impurity snake

- Nonlinear MHD simulations with toroidal rotation and separate temperature and density evolution find a **new nonlinear, slowly growing $m/n=1/1$ kink-like mode** over $q \lesssim 1$ compatible with C-Mod early snake.
- Quasi-steady-state **helical density perturbation peaks near $q=1$** and extends outside $q \gtrsim 1$.
- **Helical temperature $\delta T \approx -\delta n$ tends to minimize the perturbed pressure gradient** (ie, free energy) at $q \approx 1$, somewhat at $q < 1$.
- No initial magnetic island; forms slowly
- 1/1 kink motion is perpendicular to main density near $q=1$ so **density snake would not be affected by the sawtooth crash.**
- Background toroidal rotation important



Helical δT tends to become anti-aligned with δn



- n , T , p for parallel density helicity and toroidal rotation
 - a) At $q \approx 1$, helical $n=1$ δT (contour lines) is anti-aligned with δn (red/blue shaded). Inside $q < 1$, δn is small. (Shown in plane $\varphi = \pi/2$ where density peak on $q=1$ lies on outboard midplane.)
 - c) Midplane profiles for a).
 - b) δT (shaded) is almost aligned with δp (lines) and $\delta \psi$ (at $\varphi \approx 0$).
- Mode rotates toroidally with background rotation.

Summary

- Compressibility and finite aspect ratio corrections in the $m=1, n=1$ MHD internal kink mode remove many inconsistencies with sawtooth experimental observations
 - Nonlinear MHD: “X” reconnection region, not Sweet-Parker layer! Fast crash phase with fast onset; rate nearly independent of η . Two-fluid acceleration not needed.
 - Large aspect ratio expansion breaks down at small $r_1/R \approx 1/10 \Rightarrow$ Important implication for plasma edge instabilities!
- Compressibility \leftrightarrow evolving dn/dt
 - New type of nonlinear 1/1 mode with a finite size density perturbation at $q=1$ resembles the early stage of heavy-impurity ion snakes in Alcator C-Mod
- 1/1 work continuing - also 1/1 electron fishbones
- Future: Small amount of high-Z impurities can be important for MHD instabilities (charge density $\delta n_e, \delta p$ or P_{rad} cooling/ η). ITER will have tungsten with $Z=74$!

Other News – M3D, NERSC

- NERSC Edison/Hopper: problems porting M3D to Edison
 - Potential problem with PETSc 3.3 and M3D: strange run-time memory errors (Josh Breslau and me, independent upgrades); working with NERSC consultants and PETSc group
 - PETSc 3.1 works fine (Hopper) but only 3.3 on Edison
 - Edison: only cray-compiler works with mixed Fortran/C and PETSc, but problems with M3D
- NERSC visualization
 - New NX server doesn't support full Mac screen resolution on laptop Retina display.
 - If you miss Euclid, the old dedicated viz machine, tell NERSC now!
- Many changes being considered at NERSC – your input wanted!